博 士 論 文

A study on the differentiation potential of human bone marrow-derived mesenchymal stem cells under xeno-free culture condition
(動物由来成分を含まない培養条件による骨髄由来間葉系幹細胞の分化能に関する研究)

令和　6年　3月申請

北海道大学
大学院歯学院口腔医学専攻

渡　辺　陽　久

A study on the differentiation potential of human bone marrow-derived mesenchymal stem cells under xeno-free culture condition

Haruhisa Watanabe[1, 2] and Tadahiro Iimura[2]

[1] Departments of Oral Medicine and Diagnostics, and [2] Pharmacology, Faculty and Graduate School of Dental Medicine, Hokkaido University

N13 W7, Sapporo 060-8586, Japan

Abstract

Mesenchymal stem cells (MSCs) exhibit diverse differentiating abilities. In oral and maxillofacial surgery, bone marrow-derived MSCs (BMMCSs) are explored for treating jaw and alveolar bone regeneration. To obtain enough amount of MSCs for regenerative therapies, cell population is needed to be expanded in cell culture media. Conventional cell culture media contain animal-derived serum (Xeno-media), which leads to concerns related to xenogenic response and animal-derived pathogens. To solve these concerns, xeno-free culture media has been developed. However, it is still largely unknown whether xeno-free media has equivalent effects as xeno media on MSCs. This study compared the effects of xeno and xeno-free media on human BMMSCs. BMMSCs cultured in the xeno-free conditions showed promoted osteogenic and suppressed adipogenic capacities compared to those in the xeno condition. The xeno-free group of cells exhibited homogenous cell

morphology with fissional mitochondria, while the xeno group of cells was morphologically heterogenous with fusional mitochondria. Gene expression analysis by RT-qPCR of stem cell and differentiation markers did not show significant differences between these groups. Therefore, these results suggested pivotal roles of metabolic alterations in differentiation potentials of BMMSCs.

Introduction

Mesenchymal stem cells (MSCs) are multipotent stem cells found in several mesenchymal tissues throughout the human body, which have potentials to generate bone, cartilage, fat, fibroblasts, and vascular support cells such as pericytes and vascular smooth muscle cells[1-3]. The sources of MSCs involve bone marrow, umbilical cord tissue, adipose tissue, dental tissues such as dental pulp and periodontal ligament, and amniotic fluid. Bone marrow is the tissue where MSCs are originally discovered, and is still the most frequently utilized source. However, bone marrow loses its potential to support bone marrow-derived MSCs (BMMSCs) that are deplete with age and after disease. The depletion of multipotency of BMMSCs often correlates with the increase in adiposity. This is one major reason bones fail to regenerate with age and after age-related diseases such as osteoporosis. Bone marrow-derived MSCs (BMMSCs) act not only as multipotent stem cells but also as potent microenvironmental modulators that exert enormous anti-inflammatory effects after systemic transplantation, which benefit diverse tissues/organs, including bone[3].

Currently, MSCs-based bone and dental regeneration mainly includes two strategies: rescuing or mobilizing endogenous MSCs and applying exogenous MSCs as cytotherapy and tissue engineering, respectively[3]. Within recent decades, the transplantation of exogenous MSCs through different routes has been widely explored in bone and dental regenerative medicine. A promising strategy is the systemic application via primarily intravenous infusion and intraperitoneal delivery, which exerts therapeutic effects on various disorders, including osteoporosis, bone fracture, osteoarthritis, and jaw osteonecrosis. Local applications of BMMSCs have been well studied, especially in the field of dentistry. BMMSCs with hydroxyapatite and tri-calcium phosphate heal successfully in Swine[4]. BMMSCs-based cell sheets have been successfully used to promote bone regeneration in defects and strengthen implant bone bonding[3]. For example, transplantation of BMMSCs enhanced socket healing after tooth extraction, which treatment for alveolar ridge augmentation is expected as an alternative to bone grafting[5].

The cell culture medium is essential for expansion of MSCs for regenerative medicine. Classically, fetal bovine serum (FBS) has been supplemented with growth media as a stem cell culture aid. However, for the purpose of MSCs-based therapies, there has been an increasing demand to replace animal-derived components with non-animal-derived substances, leading to the development of an xeno-free media to avoid the risks resulting from the xenogeneic origin and animal-derived pathogens of FBS[6]. Xeno-free media have been developed and

commercialized to satisfy the demands for acquiring enough amount of pathogen-free MSCs for human clinical applications. In developing Xeno-free media, extracellular matrices (ECMs) that facilitate MSCs to adhere and grow *in vitro* can be critical supplements. Currently, human-originating collagen, fibronectin, vitronectin, and active fragments of laminins have been provided for expansion of human stem cells, including human induced pluripotent stem cells and human embryonic stem cells[7-10]. Seeing back to *in vivo* bone marrow environment, spatiotemporal regulation of BMMSCs interacting with distinct types of vessels have been proposed[11], suggesting critical roles of extracellular microenvironment through ECMs in supporting BMMSCs. Since ECMs have their own bio-activity, there is still uncertainness in the influences of xeno-free media on MSCs. Recent findings have elucidated that changes in subcellular shapes of mitochondria are highly associated with differentiation of MSCs[12-14]. However, it has not yet been well studied how the changes in mitochondrial shapes affect multipotency of BMMSCs. The scope of this study is to compared the effect of commercially available serum-containing (Xeno) and xeno-free medium on multipotency of hBMMSCs by focusing on their osteogenic and adipogenic potentials, cellular growth and adhesiveness, and mitochondrial shapes.

Materials and Methods

Initial expansion of human bone marrow-derived mesenchymal stem cells

Iliac bone marrow-derived Human mesenchymal stem cells (hBMMSCs) were obtained from Lonza (Morrisville, U.S.A.). (POIETICS™ hMSC Donor 42368,). For initial cell expansion (Passage 1), hBMMSCs were cultured in StemFit for MSC (Ajinomoto, Japan), a serum-free and xeno-free culture medium for mesenchymal stem cells. Four μL of 0.5mg/μL iMatrix-511 (Matrixome, Osaka, Japan), recombinant laminin 511 E8 fragments were premixed into 10mL Stemfit for cell adhesion. hBMMSCs were cultured at 37℃ in 5% CO2 humidified air. For the second seeding step (Passage 2), cells were detached from the culture dishes using 3ml of ACCUMAX (Innovative cell technologies, Inc, San Diego, CA, U.S.A). hBMMSCs in Passage 2 were used for the following assays and observations either in MSC GM Mesenchymal Stem Cell Growth Medium BulletKit™(Lonza, Morrisville, U.S.A.), namely xeno medium, or in Stemfit (Ajinomoto Co., Inc. AminoScience Division, Tokyo Japan), namely xeno-free medium.

Expansion of hBMSCs in the xeno and xeno-free media.

Expanded hBMMSCs (Passage 2) were seeded onto ibidi μ-slides 8well (Ibidi GmbH, Germany), 96-well plate (Thermofisher Scientific, Massachusetts, U.S.A.) , 24-well (Thermofisher scientific, Massachusetts, U.S.A.) plates for the following analyses. To prepare the xeno-free medium group, these culture plates were

precoated with Imatrix511 at 0.25μg/cm^2 at 4℃ overnight diluted in PBS (-).

hBMMSCs were cultured in StemFit for MSC. For the xeno medium group, MSC GM Mesenchymal Stem Cell Growth Medium BulletKit was used as a culture medium without any ECM coating.

Proliferation assay

hBMMSCs were seeded at 5 × 10^3 per well into 96-well plates containing 200 μL culture medium per well. Cell proliferation was analyzed using a Cell Counting Kit (CCK)-8 (Donjindo Laboratories, Kumamoto, Japan). This assay was performed at 6hrs, 24hrs, 72hrs, 120hrs, 168hrs, 288hrs, and 384hrs after the seeding.

Differentiation of human bone marrow-derived mesenchymal stem cells

hBMMSCs (second passage) were seeded at 5×10^3 per well into ibidi μ-slides 8well (Ibidi GmbH, Germany) or 96well plates either in the xeno or the xeno-free media. Cells were reached subconfluent states on 7days after the seeding, and were then induced to osteoblasts and adipocytes by replacing differentiation media of MSCgo™ Rapid Osteogenic Differentiation Medium (Sartorius, Göttingen, Germany)and MSCgo™ Adipogenic Differentiation Medium (Sartorius, Göttingen, Germany), respectively. Cells were cultured in the osteogenic medium for 5 days and 10 days, and in the adipogenic medium for 14 days and 21 days and subjected to evaluate differentiation potentials as follows.

Evaluation of osteogenesis

Quantitative enzymatic activity of alkaline phosphatase (ALP), a typical osteoblastic marker, was conducted in the 96well plates cultured hMSC, using LabAssay ™ ALP (Wako Pure Chemicals, Osaka, Japan) according to the manufacturer's instructions. Specific absorbance was measured at 415nm using a Model 550 Microplate Reader (Bio-Rad, California, USA). For microscopic observation of ALP-positive osteoblasts, ALP staining was carried out in the ibidi µ-slides 8well culture wells using TRAP/ALP Stain Kit (Wako Pure Chemicals, Osaka, Japan). The ALP premix substrate solution was put at 200µl per well, and the plate was incubated at 37℃ for 1hr. After removing the ALP premix substrate solution, the wells were washed thoroughly with PBS (-) two times and then observed immediately under bright field microscopy.

Evaluation of adipogenesis

Adipogenesis of hBMMSCS was evaluated with an Oil Red O Stain Kit (ScyTek laboratories, Utah, USA). We put 100µL per well of Propylene Glycol for 5 minutes. Incubate plates in heated (60℃) Oil Red O solution for 8 minutes in a preheated oven at 60℃. After removing the Oil Red O solution, we put 200µL of 85% Propylene Glycol for 1 minute to differentiate the tissue section. Then, we rinsed thoroughly with 200µL per well of distilled water and stained cells with Hematoxylin, Mayer’s (Lillie’s Modification) for 1 minute at room temperature. The solution was taken thoroughly and rinsed wells four times at 200µL of distilled water. PBS (-)

was added. The number of Oil Red O-positive adipocytes was scored and statistically compared under bright field microscopy manually.

Evaluation of hBMMSCs morphology and their mitochondrial morphology

hBMMSCs were seeded at 5×10^3 per well into the ibidi μ-slides 8well (Ibidi GmbH, Gräfelfing, Germany). After 3, 6 hours, one day, and seven days of the cell culture, immunostainings were conducted.

Immunofluorescence staining

hBMMSCs were fixed with 4% paraformaldehyde phosphate buffer solution and washed with PBS, permeabilized in 0.2% Triton X-100/PBS, and stained using Anti-Vinculin Antibody, clone VIIF9 (7F9) Ascites Free (Product code MAB3574-C, Merck KGaA, Darmstadt, Germany) as primary antibodies at 1:200 in 1% bovine serum albmin in TBST for 1.5 h at room temperature followed by incubation with Goat Anti- Mouse IgG (H+L) antibody Alexa Fluor 488(Cat. No. A11029, Thermofisher scientific, Massachusetts, U.S.A.) as secondary antibodies for 1 h at room temperature.

To observe mitochondria, anti-TOM20 antibody (Cat. no. sc-11415, Santa Cluz Biotechnology, Texas, U.S.A.) at 1:50 in 1% bovine serum albumin in TBST for1.5 h at room temperature was used as a primary antibody, followed by incubation with Goat Anti-Rabbit IgG (H+L) Alexa Fluor 488 (Cat.no. A11008, Thermofisher scientific, U.S.A.) as a secondary antibody for 1h at room temperature.

As counter-staining, cells were incubated with Alexa Fluor 568 Phalloidin(Cat. no. A12380, Thermofisher Scientific, Massachusetts, U.S.A.) and DAPI (Product code D523, Dojindo, Kumamoto, Japan) for staining of actin filaments and nuclei, respectively, for 30 minutes at room temperature.

Confocal microscopy

Fluorescence imaging was obtained using a microscopy system, ECLIPSE Ti2 (Nikon, Tokyo, Japan), equipped with (Nikon, Tokyo, Japan) Plan Apo VC 20×DIC N2 (NA=0.75) and Plan Apo ID ×60 Oil (NA = 0.95). The frame size of a single scan was 1024 × 1024 pixels, with a 12-bit color depth. The fluorescence images were sequentially acquired, with a pixel size of 0.62px/μm for ×20 and 0.41 μm/px for ×60. Image processing was performed using the NIS-Elements AR imaging software program (Nikon, Tokyo, Japan).

qPCR analysis

hBMMSCs were seeded into 24-well plates at density 2.0×10^5cells/well. After seven days of culture at 37℃ in 5% CO2 humidified air, total RNA was extracted with Rneasy Mini Kit (QIAGEN, Hilden, Germany) and reverse-transcribed into first-strand cDNA using a ReverTra Ace qPCR RT Master Mix (TOYOBO, Siga, Japan) according to the manufacturer's instructions. RT-qPCR was performed with THUNDERBIRD™ Next SYBR® qPCR Mix (TOYOBO, Siga, Japan) and Eco™

Real-Time PCR System (Illumina, Tokyo, Japan). All sequences for primers used in this study are provided in Table 1. Relative expression to RPLP0 was examined using the $2^{-\Delta\Delta Ct}$ method.

(Table1)

	Forward	**Reverse**
Reference gene		
RPLP0	TGGTCATCCAGCAGGTGTTCGA	ACAGACACTGGCAACATTGCGG
Undifferentiation marker		
Oct4	CCTGAAGCAGAAGAGGATCACC	AAAGCGGCAGATGGTCGTTTGG
NANOG	CTCCAACATCCTGAACCTCAGC	CGTCACACCATTGCTATTCTTCG
Osteogenic marker		
Sp7	TTCTGCGGCAAGAGGTTCACTC	GTGTTTGCTCAGGTGGTCGCTT
RUNX2	CCCAGTATGAGAGTAGGTGTCC	GGGTAAGACTGGTCATAGGACC
Chondrogenic marker		
SOX9	AGGAAGCTCGCGGACCAGTAC	GGTGGTCCTTCTTGTGCTGCAC
Adipogenic marker		
PPARγ	AGCCTGCGAAAGCCTTTTGGTG	GGCTTCACATTCAGCAAACCTGG
MSCs characterization marker		
LEPR	GCAGTCTATGCTGTTCAGG	CCAAAATTCAGGTCCTCTCA

	TGC	TAGG
CXCL12	CTCAACACTCCAAACTGTGCCC	CTCCAGGTACTCCTGAATCCAC
PDGFRB	TGCAGACATCGAGTCCTCCAAC	GCTTAGCACTGGAGACTCGTTG
Tryptophan metabolic pathway marker		
IDO1	GCCTGATCTCATAGAGTCTGGC	TGCATCCCAGAACTAGACGTGC
TPH1	CTGCAGCATGATCTCGATGT	ATTGTTTGGCCAGAAGATGC
Lysine metabolic pathway marker		
AASS	GGCTTCTTGGTGGCAAAACAGG	GCTGGTGTGATGTAGCTTGCAG
ALDH7A1	GGCTTCTTGGTGGCAAAACAGG	GCTGGTGTGATGTAGCTTGCAG

Statistical analysis

The data are presented as the mean ± standard deviation (SD). All statistical analysis and fabrication of graphs were performed using GraphPad Prism (ver.10.1.0). We set statistical significance at $p<0.05$. Two-way ANOVA was conducted, followed by an uncorrected Fisher's LSD test analysis performed as a post-hoc test for multiple comparisons.

Results

Cell proliferation assay

To evaluate the influences of the xeno and xeno-free growth media on hBMMSCs proliferation, we first conducted cell proliferation assay at distinct time points after the initial seeding (Figure1). Up to 288 hours, the xeno medium group showed significantly faster proliferation rates than that in the xeno-free medium group. However, at 384 hours, the cell numbers in the xeno medium group suddenly decreased, while cells in the xeno-free medium group still stably maintained their cell number. Based on these findings, we decided to subject the BMMSCs expanded under the xeno and xeno-free growth media for 7 days to differentiation assays.

(Figure 1)

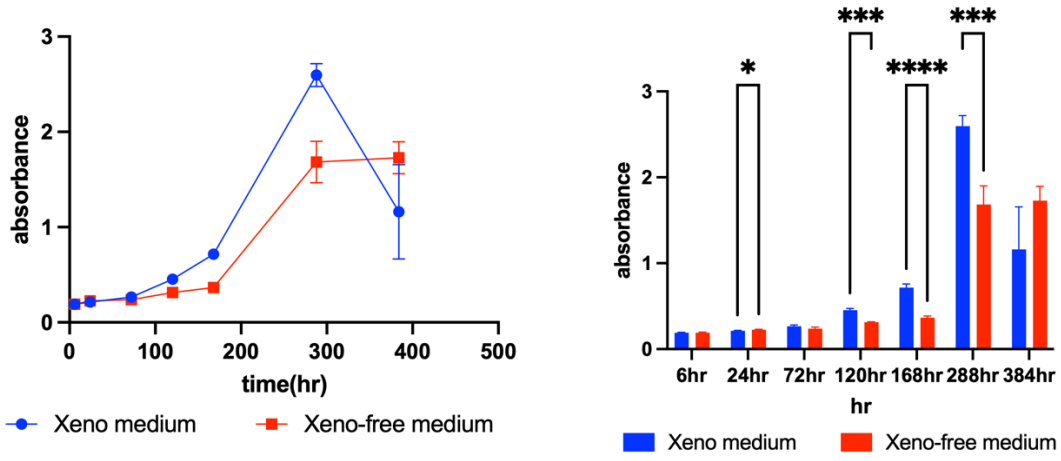

Figure 1. Cell growth analyses

Relative numbers of hBMMSCs cultured in the xeno, and xeno-free media were counted with CCK-8 assay at indicated time points, and statistically compared.

n=4,Two-way ANOVA, Uncorrected Fisher's LSD test as a post-hoc test

*p<0.05,***p<0.001,****p<0.0001

Osteogenic differentiation assay

To evaluate osteogenic potentials of two groups of hBMMSCs expanded under the xeno and xeno-free growth media for 7 days, enzymatic activity and cellular staining assays of ALP were conducted on these two distinct groups of cultured cells under osteogenic media for 5 and 10 days after the osteogenic induction (Figure 2). The enzymatic activity assay showed significantly promoted osteoblast differentiation in the xeno-free medium group compared to that in the xeno medium group on 5 and 10 days after differentiation induction (Figure 2, left). Consistently, the ALP staining assay showed more intense staining of ALP-positive cells observed in the xeno-free medium group than those in the xeno medium group (Figure 2, right). These findings suggested that the expanded cells under the xeno-free medium have enhanced osteogenic potential compared to those expanded under the xeno medium.

(Figure2)

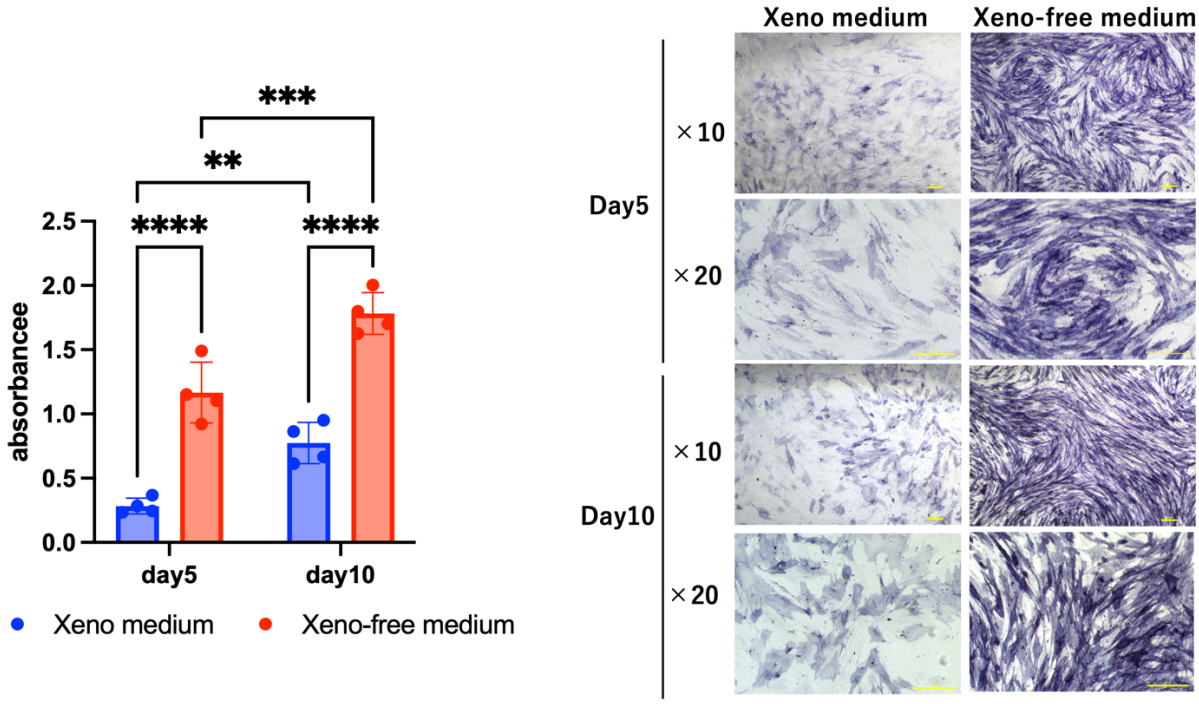

Figure 2. Evaluation of osteogenic potential using ALP staining

Osteogenic potentials of hBMMSCs cultured in the xeno, and xeno-free media were compared with the enzymatic activities of ALP (left), and with celluar ALP-staining (right) at indicated time points. Scale bars=200μm

n=4, Two-way ANOVA, Uncorrected Fisher's LSD test as a post-hoc test

p<0.01,*p<0.001,****p<0.0001

Adipogenic differentiation assay

To evaluate adipogenic potentials of two groups of cells expanded under xeno and xeno-free growth media for 7 days, Oil-Red O staining assays were conducted on these two distinct groups of cultured cells under adipogenic media for 14 and 21

days after adipogenic induction (Figure 3). The number of Oil-Red O-positive adipocytes was significantly reduced in the xeno-free medium group compared to that in the xeno medium group on 14 and 21 days(Figure 3, left). Microscopic observations demonstrated that fewer and smaller Oil-Red O-positive cells were seen in the xeno-free medium group than those in the xeno medium (Figure 3, right). These findings suggested that the expanded cells under the xeno-free medium have suppressed adipogenic potential compared to those expanded under the xeno medium.

(Figure3)

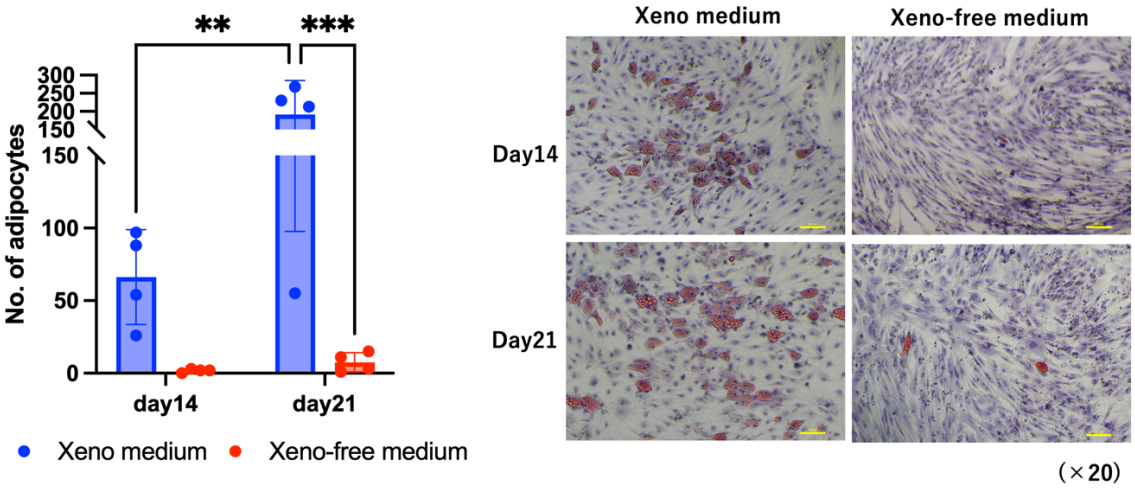

Figure 3. Evaluation of adipogenic potential using Oil Red O staining

Adipogenic potentials of hBMMSCs cultured in the xeno, and xeno-free media were compared with the Oil Red O staining. The number of Oil Red O-positive cells at indicated time points were counted and statistically compared (left) of enzymatic activities of ALP (left), and with cellular ALP-stainings (right). Oil Red O-

positive cells counterstained with Hematoxylin-Eosin were shown (right).
Scale bars=100μm, n=4, Two-way ANOVA, Uncorrected Fisher's LSD test as a post-hoc test
p<0.01,*p<0.001

Cellular morphology

To evaluate the influences on cellular morphology by xeno and xeno-free growth media, we first conducted immunofluorescence with anti-Vinculin antibodies to visualize focal adhesion points. The hBMMSCs were also counter-stained with phalloidin and DAPI to see actin fibers and nuclei, respectively, and observed stained hBMMSCs at 3 and 6hours, on 1 and 7 days after the initial seeding on culture dish. At 3 and 6 hours after the initial culture, cells in the xeno medium group showed relatively small and round shapes with focal adhesions on their peripheries, while, in the xeno-free medium group, cells extended their bodies with well-developed lamellipodia, filopodia and actin fibers (Figure 4a, b). At 6 hours, cells on the both groups more widely extended their bodies compared to those at 3 hours (Figure 4b). On 1 day after the culture, cells on the both groups showed their polygonal and spindle shapes. Cells in the xeno medium groups still looked smaller than those in the xeno-free medium group (Figure 4c). On 7 days, the tendencies of cell sizes appeared to be reversed; cells in the xeno medium group showed larger sizes than those in the xeno-free medium group. Consistently, more intense stress fibers and focal adhesions can be seen in the xeno medium group

compared to those in the xeno-free medium group (Figure 4c). Notably, in the xeno-free medium group, cell shapes became homogeneously spindle, while cells in the xeno medium group showed heterogeneity both in shape and size (Figure 4d).

(Figure 4a)

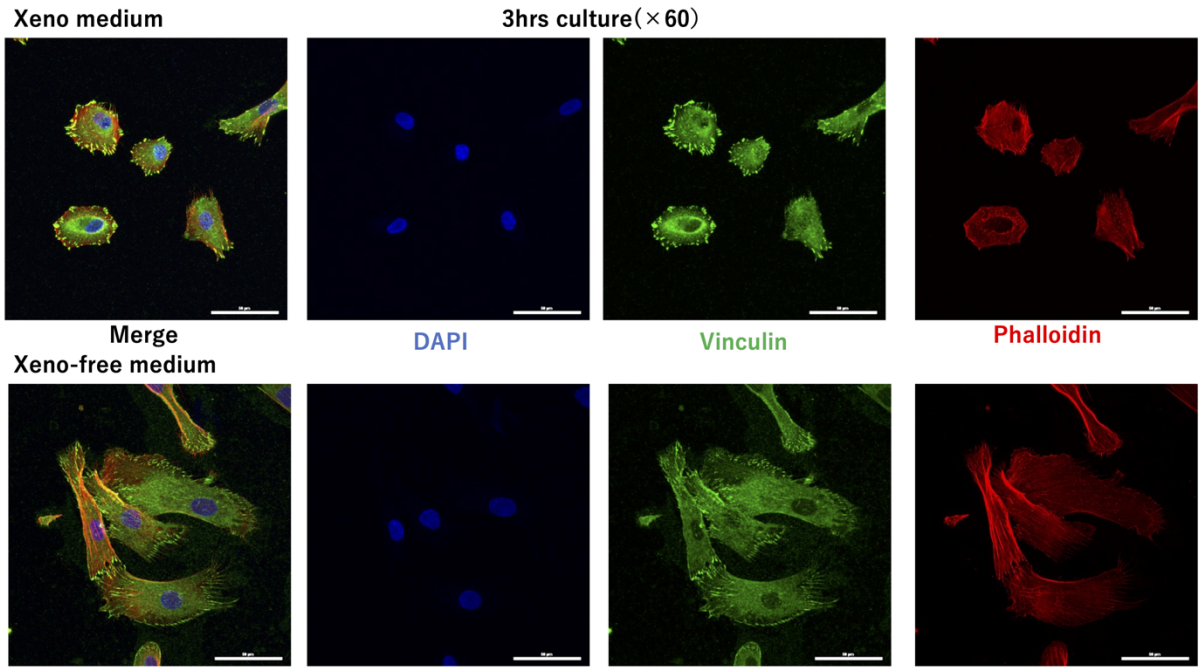

(Figure 4b)

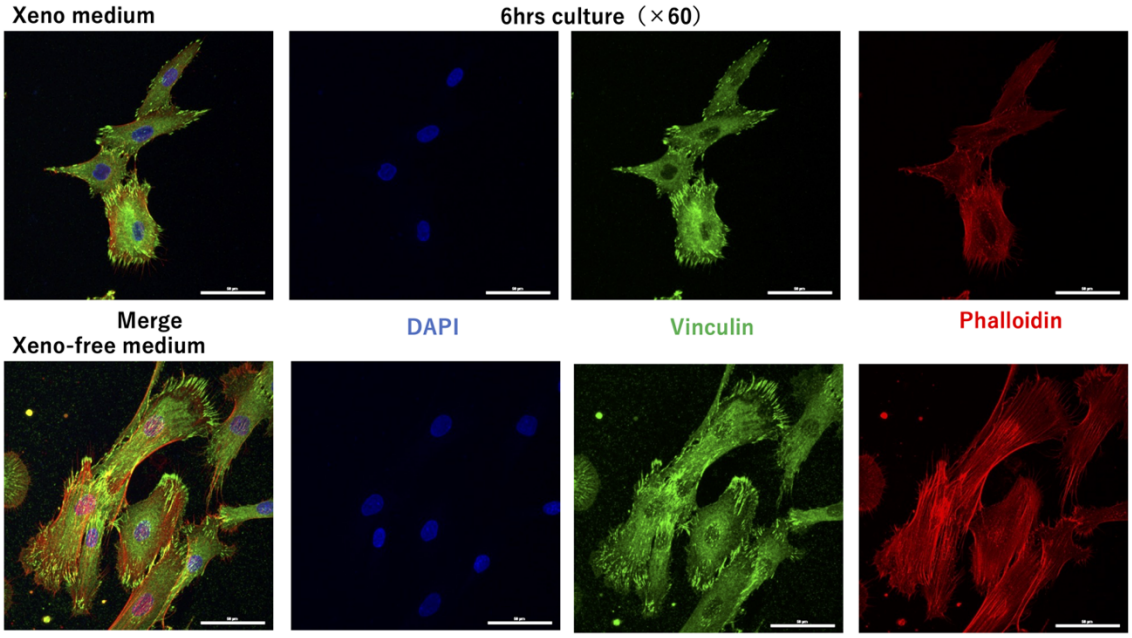

(Figure 4c)

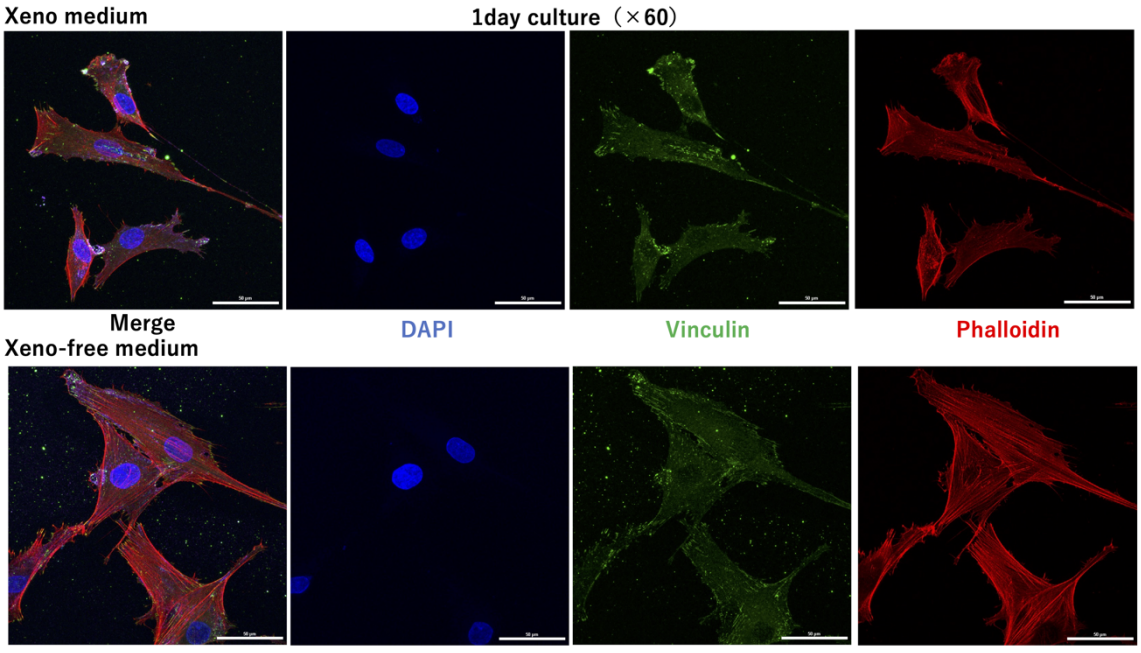

(Figure 4d)

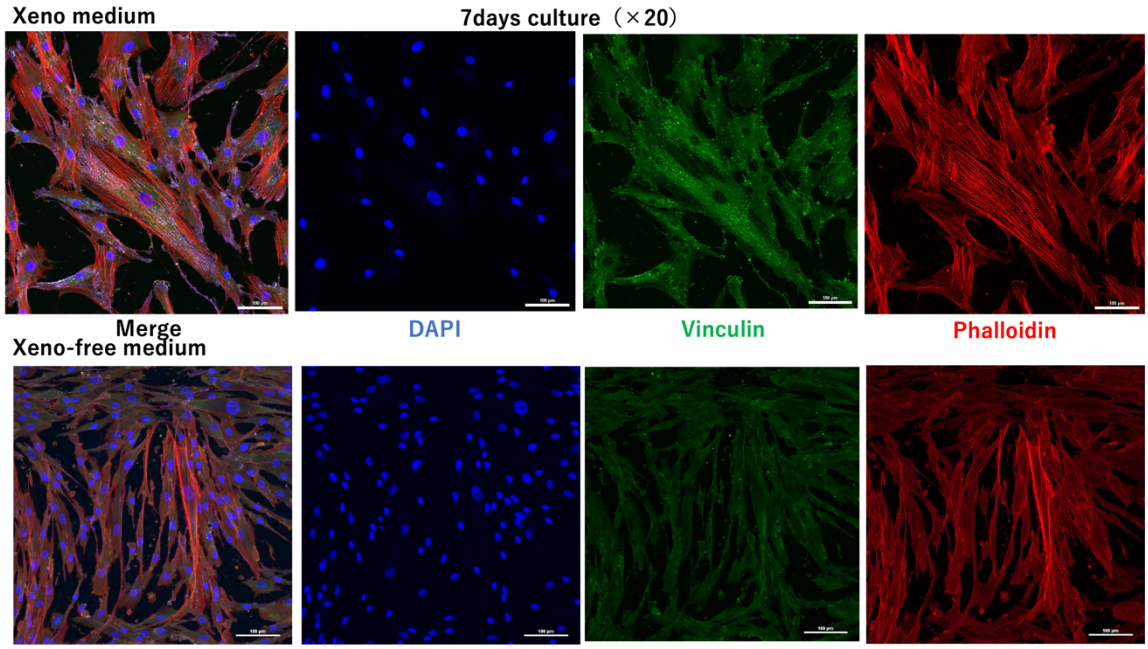

Figure 4. Evaluation of celluar structure

Cellular structures of hBMMSCs cultured in the xeno, and xeno-free media were compared at 3, 6 h and 1, 7 days after culture (a, b, c, and d, respectively). Upper and lower panels show hBMMSCs in the xeno, and xeno-free media, respectively. Cells were immunostained with anti-Vinculin antibodies counter stained with DAP and Phalloidin for marking nuclei and actin fibers, respectively. Scale bars=50μm in figure 4a,4b,4c. Scale bars=100μm in figure 4d

Mitochondrial morphology

Accumulated findings have demonstrated that morphological changes affect differentiation potentials of stem cells, including BMMSC (Figure 5). Therefore, we compared subcellular morphology of mitochondria on 1 and 7 days after the initial

seeding. On 1day, in the xeno medium group, mitochondrial subcellular networks looked widely extended to whole cytoplasm with their linear and fusional shapes, while mitochondrial networks in the xeno-free medium group tended to accumulate surrounding nuclei with fissional, fragmented, or round-shaped mitochondria predominantly observed in cellular periphery (white arrow in figure 5a). These characteristic features of mitochondrial subcellular morphology in both groups were maintained up to 7 days after the culture, even though characteristics in cell sizes were reversed (Figure 5b and c).

(Figure 5a)

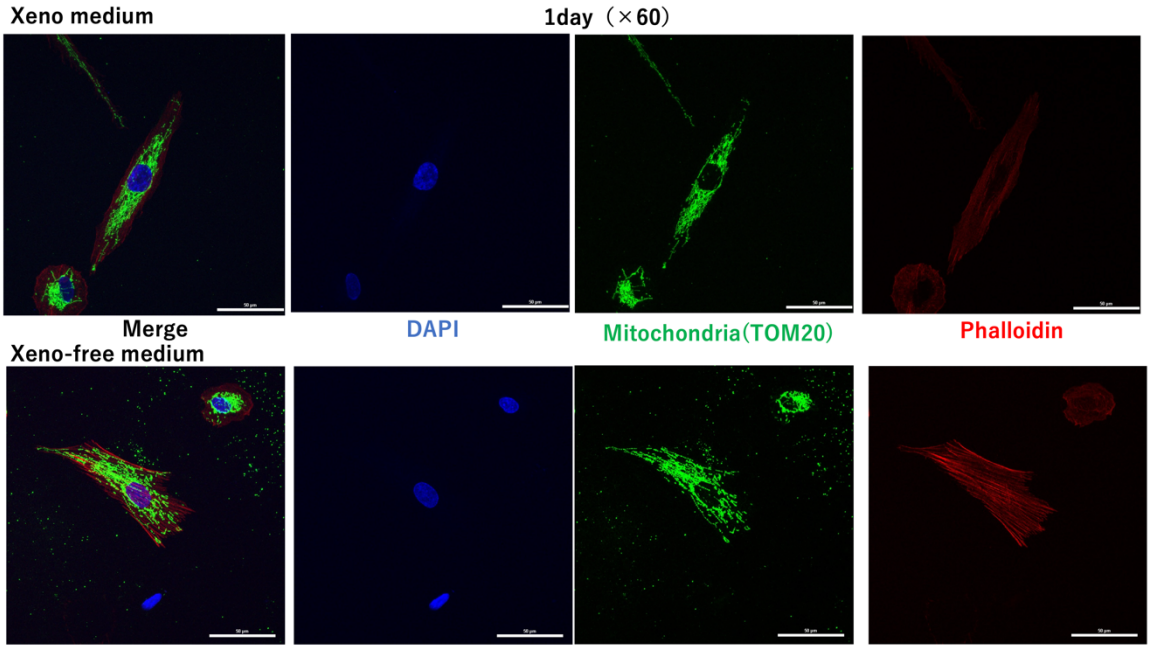

(Figure 5b)

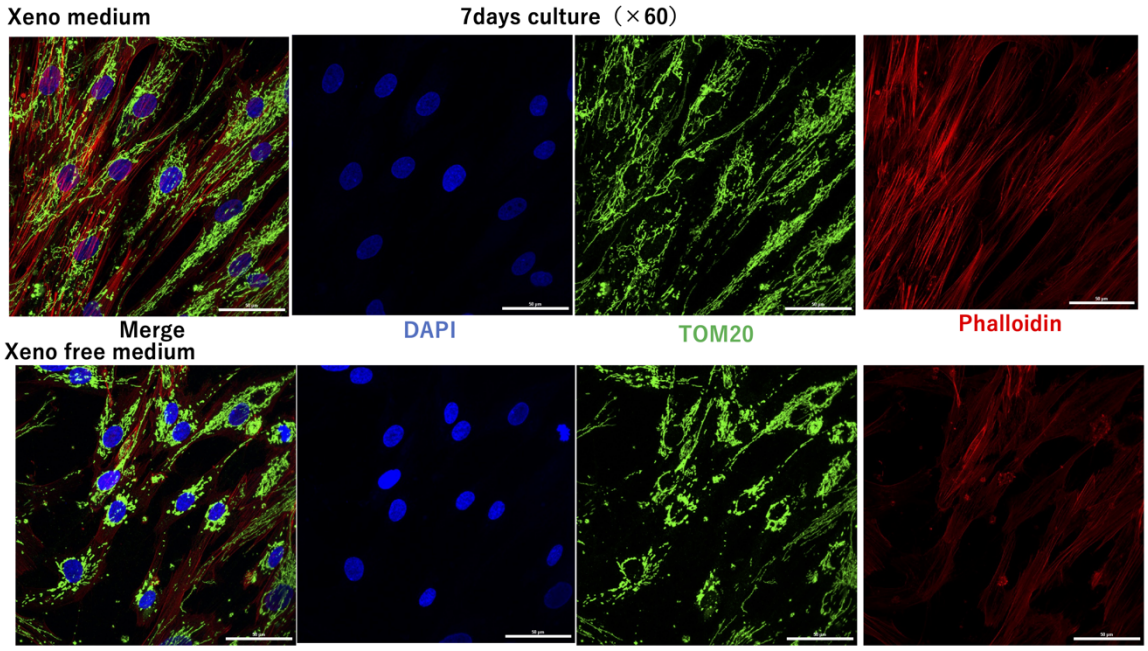

(Figure 5c)

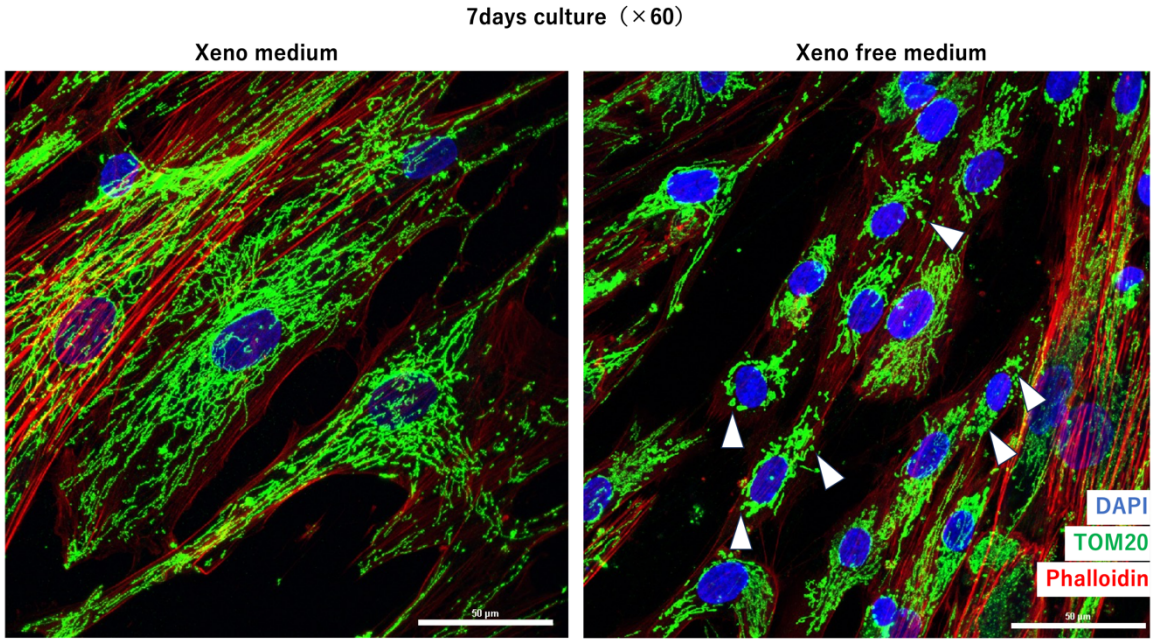

Figure 5. Evaluation of mitochondrial morphology

Mitochondrial morphologies of hBMMSCs cultured in the xeno, and xeno-free media were compared on 1 day (a), and 7 days (b, c) after culture. Upper and lower panels and show hBMMSCs in the xeno, and xeno-free media, respectively (a,b). Cells were immunostained with anti-TOM-20 antibodies counter stained with DAP and Phalloidin for marking nuclei and actin fibers, respectively. Magnified views of cells on day 7 are shown (c). Scale bars=50μm

Marker gene expression analyses

To find rationale of distinct differentiation potentials of two groups of cells, we compared gene expressions in cells expanded under the xeno and xeno-free media for 7days (Figure6). We did not observe significant differences in transcriptional levels of undifferentiated markers such as *NANOG* and *Oct4*, osteoblastic markers such as *SP7* and *RUNX2*, adipogenic markers such as *PPARγ*and *ADIPOQ*, *SOX2* : a chondrogenic marker, bone marrow MSC markers such as *CXCL12*, *PDGFRβ* and *LEP*R.

Since changes in Lysine and Tryptophan metabolisms are reportedly associated with differentiation potentials of stem cells, we also compared transcriptional levels of lysine metabolism markers such as *ALDH7A1* and *AASS*, and Tryptophan metabolism markers such as *IDO1* and *TPH1*. Expression levels of *ALDH7A1* and

AASS were significantly higher in the cells cultured in the xeno-free medium group than those in the xeno medium group, while levels of *IDO1* and *TPH1* did not show significant differences between groups. These findings in gene expression analyses suggested that changes in lysine metabolism were associated with distinct differentiation potentials of two groups of cells.

(Figure6)

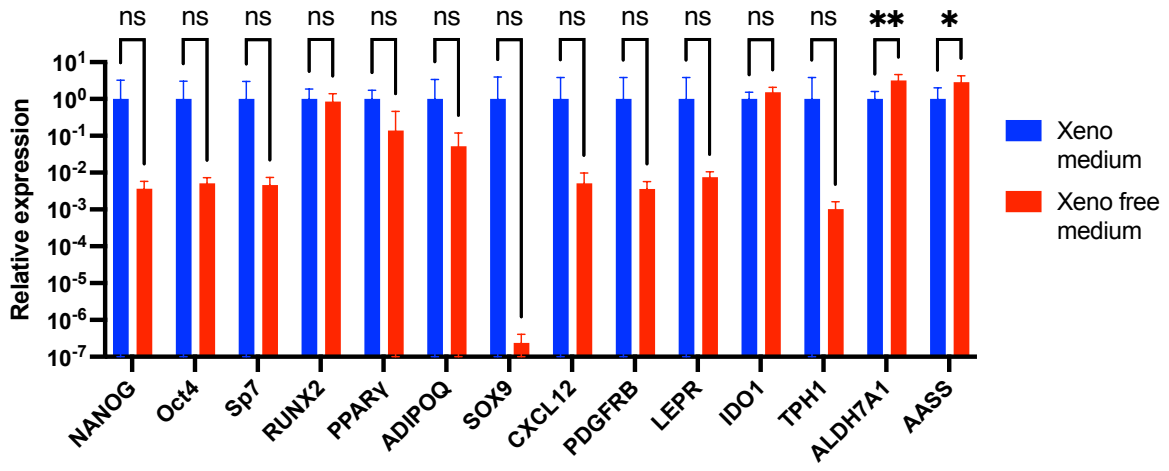

Figure 6. Comparison of transcriptional levels of marker genes

hBMMSCs cultured in the xeno, and xeno-free media on day 7 were harvested and subjected to RT-qPCR analyses. Upper and lower panels show hBMMSCs in the xeno, and xeno-free media, respectively. Cells were immunostained with anti-Vinculin antibodies counter stained with DAP and Phalloidin for marking nuclei and actin fibers, respectively. Relative expression levels of undifferentiated markers: *NANOG* and *Oct4*, osteogenic markers: *Sp7* and *RUNX2*, adipogenic markers: *PPAR* γ and *ADIPOQ*, chondrogenic marker: *SOX9*, MSC markers: *CXCL12*,

PDGFRB and *LEPR*,tryptophan metabolism markers: *IDO1* and *TPH1*, and lysine metabolism markers: *ALDH7A1* and *AASS* were statistically compared. n=9, Two-way ANOVA, Uncorrected Fisher's LSD test as a post-hoc test

*p<0.05, **p<0.01

Discussion

In this study, we compared osteogenic and adipogenic potentials of hBMMSCs that were expanded in the xeno and the xeno-free growth media. hBMMSCs proliferated under the xeno-free condition showed promoted osteogenic, but suppressed adipogenic potentials, compared to those of the cells proliferated under the xeno condition. We conducted osteogenic and adipogenic inductions on hBMMSCs expanded for 7days in the xeno or the xeno-free media. To differentiate these two groups of cells to osteoblasts or adipocytes, the same osteogenic or adipogenic media were used, respectively. Therefore, distinct differentiation potentials observed in these two groups of cells can be due to molecular and cellular events differently induced during their expansion by different growth media.

The morphology of hBMMSCs in the xeno-free group was observed to be homogenoues in their size and shape with uniformly keeping spindle shape, while the xeno group of hBMMSCs showed more heterogenous with various sizes and shapes of cells. Our observation was consistent with a previous study, which showed MSCs cultured in xeno-free/serum-free medium are more homogeneous,

smaller in size, and have a more defined spindle-shaped morphology than those cultured in FBS-supplemented medium[15].

The increase in adiposity and heterogenous populations in the xeno group of cells appeared to phenocopy senescence in MSCs. After a certain number of cell divisions, MSCs enter senescence, morphologically characterized by enlarged and irregular cell shapes and ultimately a stop their proliferation [16]. MSCs accumulate DNA damage throughout time due to growth-promoting stimuli, such as DNA replication mistakes and telomere attrition[17].

Promoted osteogenic potential in the xeno group of cells can be attributed to ECM-mediated signaling, since the xeno-free medium we used in this study uniquely contains recombinant E8 fragment of laminin 511[15] [18]. Previous study using MSCs derived from different tissue sources showed that laminin coating on culture dish promotes osteogenic induction compared with control but less osteogenic induction compared with fibronectin coating [19]. Another previous report showed that laminin coating inhibits adipogenic induction[20]. These previous findings suggest that laminin-mediated signaling played roles in differentiation potential of the hBMMSCs in the xeno-free group.

It is well-established laminins and other ECMs regulate cytoskeletal structures through their bindings to different types of integrins. Cytoskeletal regulation is highly associated with cellular morphology and cell density. Cell density and cell shapes reportedly regulate the commitment of hMSC differentiation through RhoA,

which is a target of integrin-mediated signaling[21]. This previous and our findings together suggest that ways of cellular adhesion in growth media contribute to homogenous cellular morphology and differentiation potential of hBMMSCs.

Our findings of perinuclear distribution and relatively small, round-shaped mitochondria in the xeno-free medium group may provide a prerequisite condition in favor of the osteogenic promotion. Suh et al. reported that mitochondrial fragmentation and donut formation lead to mitochondrial secretion, and the secreted mitochondria promote osteogenesis[22]. Chen et al. reported that they observed perinuclear distribution of mitochondria in the early phase of osteogenic induction, and an evenly distributed pattern was resumed after two weeks of differentiation[23]. Mitochondrial morphology and energy metabolism are also associated with pluripotency of embryonic stem cells (ESCs), induced pluripotent stem cells (iPSCs) and BMMSs[12]. Consistent with this report, the characteristics of mitochondrial morphology in the xeno-free medium group of cells in our study possibly contributed to maintaining undifferentiated states of hBMMSs. As discussed above, the morphology MSCs changes with age [24]. Another notable change of aged MSCs is senescence-associated mitochondrial dysfunction with the imbalance between fusion and fission events[17]. These previous and our findings together suggest that distinct subcellular morphology of mitochondria observed in this study is associated with distinct differentiation potential of hBMMSCs, though functional changes in mitochondrial morphology still remains to be elucidated.

Our RT-qPCR analyses did not show significant differences in transcriptional levels of stem cells or differentiation marker genes between the groups. Nevertheless, we noticed that standard deviation of any transcriptional level of these genes was higher in the xeno medium group than in the xeno-free medium group. Interestingly, Cort et al. pointed out the heterogeneity of MSCs using single-molecule RNA FISH technique[25]. Therefore, higher standard deviations of marker gene expression levels can be associated with heterogenous size and shapes in the the xeno medium group.

We also observed significantly higher expression levels of *ALDH7A1* and *AASS* in the xeno-free medium group, which suggests promoted Lysine metabolism. Reportedly, hMSCs consume amino acids during proliferation[26]. *ALDH7A1* was identified as novel susceptibility gene for osteoporosis by genome-wide study[27] . *ALDH7A1* gene encodes an enzyme of acetaldehyde dehydrogenase superfamily. These enzymes are involved in alcohol metabolism by degrading and detoxifying acetaldehyde, also affect osteogenesis, since acetaldehyde has been shown to inhibit osteoblast proliferation and decrease bone formation[28, 29] . Tryptophan metabolism, including kynurenine pathway, is also demonstrated to be involved in the function of BMMSCs [30]. Our RT-qPCR result did show significant changes in the transcriptional levels of *IDO1* and *TPH1*. These findings suggest that changes in lysin metabolism, rather than tryptophan metabolism, are associated with distinct differentiation potentials between groups.

Conclusion

This study demonstrated that expanded hBMMSCs under the xeno-free medium had promoted osteogenic and reduced adipogenic potentials compared to those expanded under the xeno medium. This difference in differentiation potential is associated with homo/heterogenous cell population, distinct mitochondrial shapes, and lysin metabolism, all of which are cellular phenotypes related to cellular senescence of hBMMCs (Figure 7).

(Figure7)

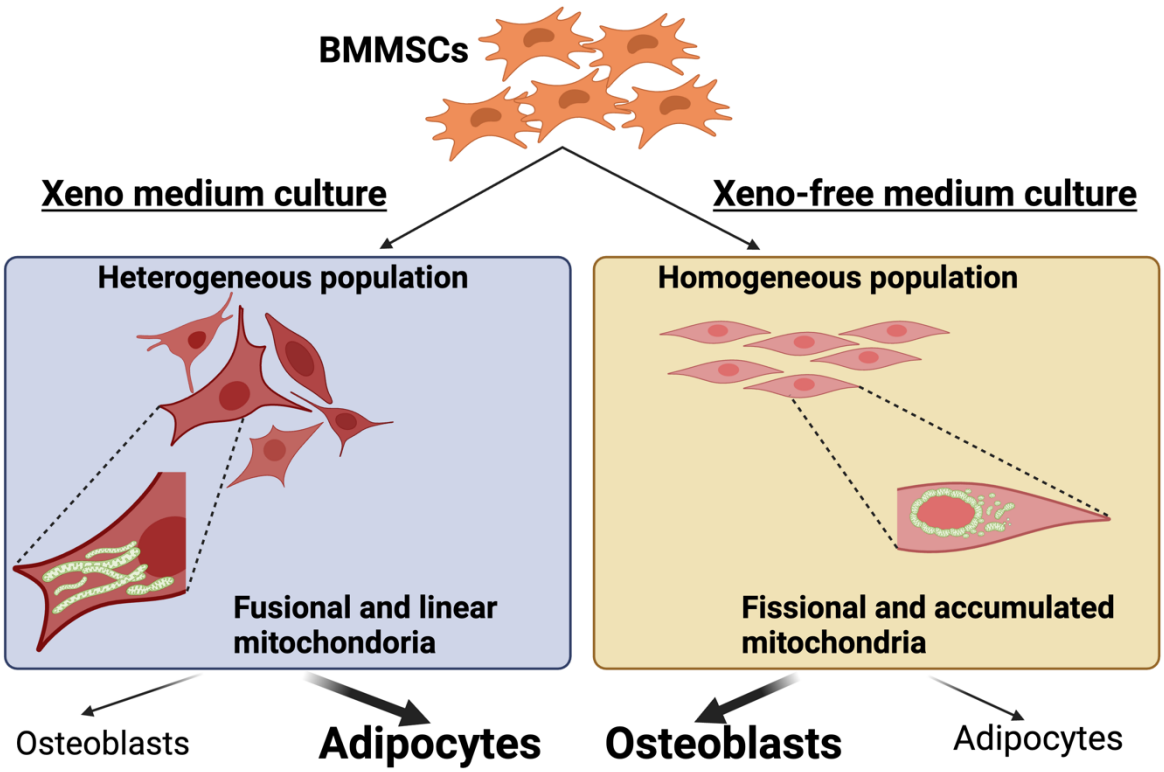

Figure 7. Schematic summary

hBMMSCs expanded in the xeno, and xeno-free media on day 7 showed differentiation potentials that favor adipogenesis and osteogenesis, respectively. These were associated with morphologically heterogenous and homogenous cell populations, with expanded, linear and fusional mitochondria and condensed, fragmented and fissional mitochondria, respectively.

Acknowledgments

We would like to express sincere thanks to Mr. Takuji Yamamoto, the President of Matrixome Cooperation, Ms. Alisa Hirota, Mr. Masashi Kusuhata, and Ms. Michi Iwai at Nippi Cooperation for their expertise in ECM biology. This work was also supported by JST SPRING, Grant Number JPMJSP2119 to H. Watanabe. We would like to thank my valued colleagues at Department of Pharmacology, and Department of Oral Medicine and Diagnostics, Faculty and Graduate School of Dental Medicine, Hokkaido University, for their constructive discussions on this research. I would also like to express my sincere gratitude to Professor Yoshimasa Kitagawa at Department of Oral Medicine and Diagnostics for his warm guidance and expertise in clinical science.

References

1. Han, Y., et al., *Mesenchymal Stem Cells for Regenerative Medicine.* Cells, 2019. **8**(8).
2. Sivaraj, K.K., et al., *Regional specialization and fate specification of bone stromal cells in skeletal development.* Cell Rep, 2021. **36**(2): p. 109352.

3. Zheng, C., et al., *Stem cell-based bone and dental regeneration: a view of microenvironmental modulation.* Int J Oral Sci, 2019. **11**(3): p. 23.
4. Xu, J., et al., *Mesenchymal stromal cell-based treatment of jaw osteoradionecrosis in Swine.* Cell Transplant, 2012. **21**(8): p. 1679-86.
5. Mashimo, T., et al., *Bone marrow-derived mesenchymal stem cells enhance bone marrow regeneration in dental extraction sockets.* J Oral Sci, 2019. **61**(2): p. 284-293.
6. Lee, J., et al., *Standard for characteristics of adipose derived stem cells cultivated with serum free defined media.* Cytotherapy, 2020. **22**(5).
7. Linsley, C., B. Wu, and B. Tawil, *The effect of fibrinogen, collagen type I, and fibronectin on mesenchymal stem cell growth and differentiation into osteoblasts.* Tissue Eng Part A, 2013. **19**(11-12): p. 1416-23.
8. Tian, Z., et al., *Effect of extracellular matrix proteins on the differentiation of human pluripotent stem cells into mesenchymal stem cells.* J Mater Chem B, 2022. **10**(30): p. 5723-5732.
9. Hynes, R.O., *Integrins: bidirectional, allosteric signaling machines.* Cell, 2002. **110**(6): p. 673-87.
10. Langen, U.H., et al., *Cell-matrix signals specify bone endothelial cells during developmental osteogenesis.* Nat Cell Biol, 2017. **19**(3): p. 189-201.
11. Watanabe, H., et al., *Skeletal-Vascular Interactions in Bone Development, Homeostasis, and Pathological Destruction.* Int J Mol Sci, 2023. **24**(13).
12. Ren, L., et al., *Mitochondrial Dynamics: Fission and Fusion in Fate Determination of Mesenchymal Stem Cells.* Frontiers in Cell and Developmental Biology, 2020. **8**.
13. Yan, W., S. Diao, and Z. Fan, *The role and mechanism of mitochondrial functions and energy metabolism in the function regulation of the mesenchymal stem cells.* Stem Cell Res Ther, 2021. **12**(1): p. 140.
14. Quinn, K.P., et al., *Quantitative metabolic imaging using endogenous fluorescence to detect stem cell differentiation.* Sci Rep, 2013. **3**: p. 3432.
15. Bui, H.T.H., L.T. Nguyen, and U.T.T. Than, *Influences of Xeno-Free Media on Mesenchymal Stem Cell Expansion for Clinical Application.* Tissue Eng Regen Med, 2021. **18**(1): p. 15-23.
16. Wagner, W., et al., *Replicative senescence of mesenchymal stem cells: a continuous and organized process.* PLoS One, 2008. **3**(5): p. e2213.
17. Weng, Z., et al., *Mesenchymal Stem/Stromal Cell Senescence: Hallmarks, Mechanisms, and Combating Strategies.* Stem Cells Transl Med, 2022. **11**(4): p. 356-371.
18. Wang, L., et al., *Integrins in the Regulation of Mesenchymal Stem Cell Differentiation by Mechanical Signals.* Stem Cell Rev Rep, 2022. **18**(1): p. 126-141.
19. Shen, C., et al., *Comparison of osteogenic differentiation capacity in mesenchymal stem cells derived from human amniotic membrane (AM), umbilical cord (UC), chorionic membrane (CM), and decidua (DC).* Cell Biosci, 2019. **9**: p. 17.
20. Novoseletskaya, E., et al., *Mesenchymal Stromal Cell-Produced Components of Extracellular Matrix Potentiate Multipotent Stem Cell Response to Differentiation Stimuli.* Front Cell Dev Biol, 2020. **8**: p. 555378.
21. McBeath, R., et al., *Cell shape, cytoskeletal tension, and RhoA regulate stem cell lineage*

commitment. Dev Cell, 2004. **6**(4): p. 483-95.
22. Suh, J., et al., *Mitochondrial fragmentation and donut formation enhance mitochondrial secretion to promote osteogenesis.* Cell Metab, 2023. **35**(2): p. 345-360 e7.
23. Chen, C.T., et al., *Coordinated changes of mitochondrial biogenesis and antioxidant enzymes during osteogenic differentiation of human mesenchymal stem cells.* Stem Cells, 2008. **26**(4): p. 960-8.
24. Al-Azab, M., et al., *Aging of mesenchymal stem cell: machinery, markers, and strategies of fighting.* Cell Mol Biol Lett, 2022. **27**(1): p. 69.
25. Cote, A.J., et al., *Single-cell differences in matrix gene expression do not predict matrix deposition.* Nat Commun, 2016. **7**: p. 10865.
26. Higuera, G.A., et al., *Patterns of amino acid metabolism by proliferating human mesenchymal stem cells.* Tissue Eng Part A, 2012. **18**(5-6): p. 654-64.
27. Guo, Y., et al., *Genome-wide association study identifies ALDH7A1 as a novel susceptibility gene for osteoporosis.* PLoS Genet, 2010. **6**(1): p. e1000806.
28. Vidal, C., et al., *The kynurenine pathway of tryptophan degradation is activated during osteoblastogenesis.* Stem Cells, 2015. **33**(1): p. 111-21.
29. Duque, G., et al., *Picolinic Acid, a Catabolite of Tryptophan, Has an Anabolic Effect on Bone In Vivo.* J Bone Miner Res, 2020. **35**(11): p. 2275-2288.
30. Pham, H.T., et al., *Tryptophan and Kynurenine Enhances the Stemness and Osteogenic Differentiation of Bone Marrow-Derived Mesenchymal Stromal Cells In Vitro and In Vivo.* Materials (Basel), 2021. **14**(1).